Confinement Effects of Metal-Organic Framework on the Formation of Charge-Transfer Tetrathiafulvalene Dimers

Ting Chen, Peng Huo, Jin-Le Hou, Jing Xu, Qin-Yu Zhu,*and Jie Dai*

College of Chemistry, Chemical Engineering and Materials Science, Soochow University, Suzhou 215123, P. R. China

Figure:

Figure S1 The experimental powder XRD patterns and the simulated patterns from the crystal data of compounds **1–3**.

Figure S2 PXRD of the freshly prepared crystals, samples kept in ambient condition for three months and after CV measurement of compounds **1–3**.

Figure S3 Raman spectra for compounds **2** and **3**.

Figure S4 The chain structure bridged by L along the b axis of $[MnL(bpp)]_n$ (**1**), bpp is omitted for clarity.

Figure S5 (a) Structure of $[Cd_2L(bpp)_2(H_2O)(C_2O_4)_{0.5}]_n \cdot n(ClO_4) \cdot n(H_2O)$ (**3**). (b) and (c) Centrosymmetric tetranuclear cluster through double μ_2-O bridges from two different L. (d) 3-D MOF structure showing that TTF dimers, perchlorate anions and water molecules are occupied in the pores.

Table:

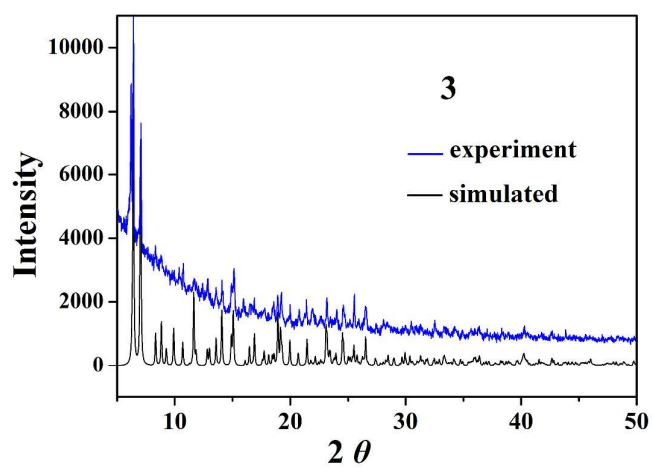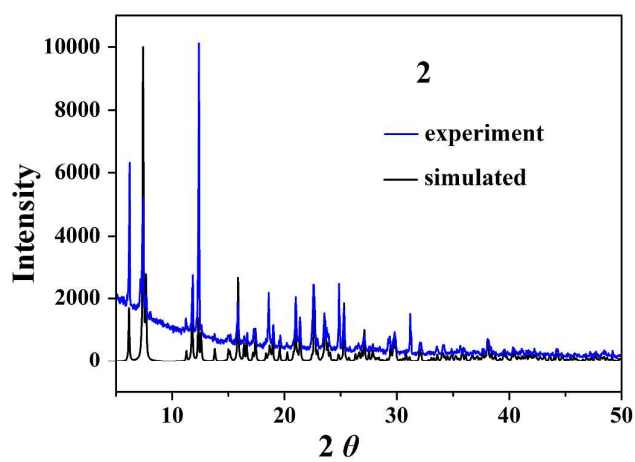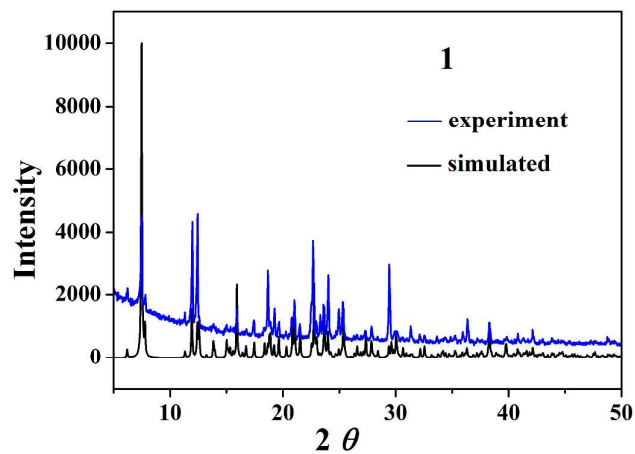Table S1. Crystal data and structural refinement parameters for **1–3**.

Figure S1 The experimental powder XRD patterns and the simulated patterns from the crystal data of compounds **1**–**3**.
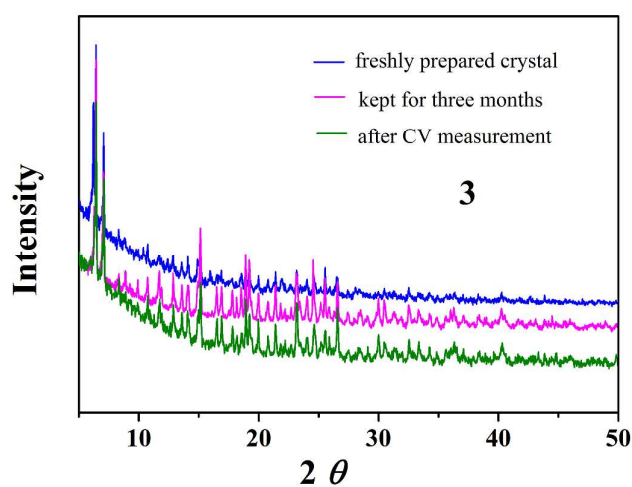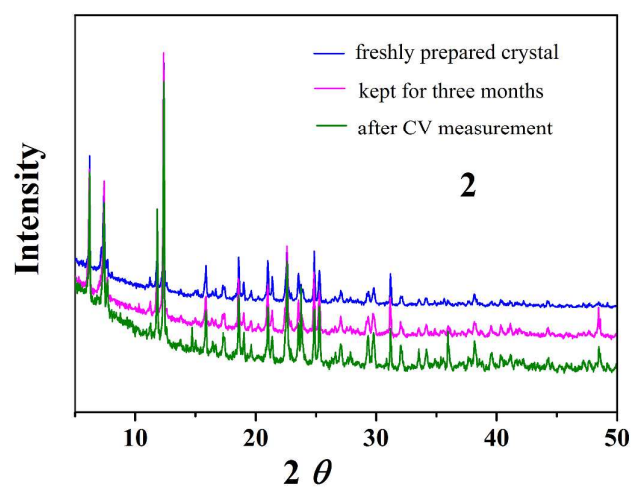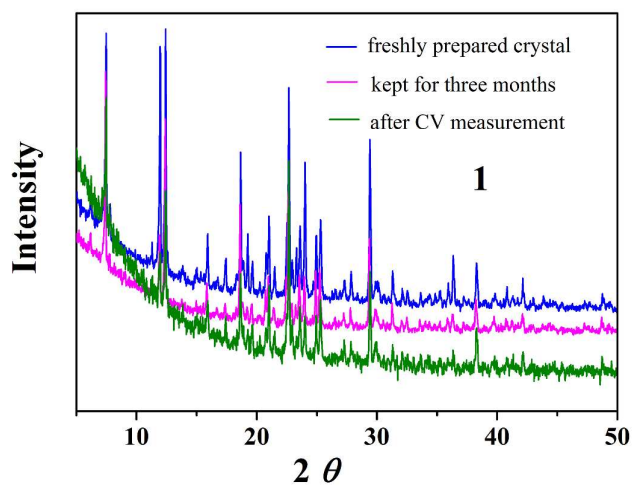
Figure S2 PXRD of the freshly prepared crystals, samples kept in ambient condition for three months and after CV measurement of compounds **1–3**.
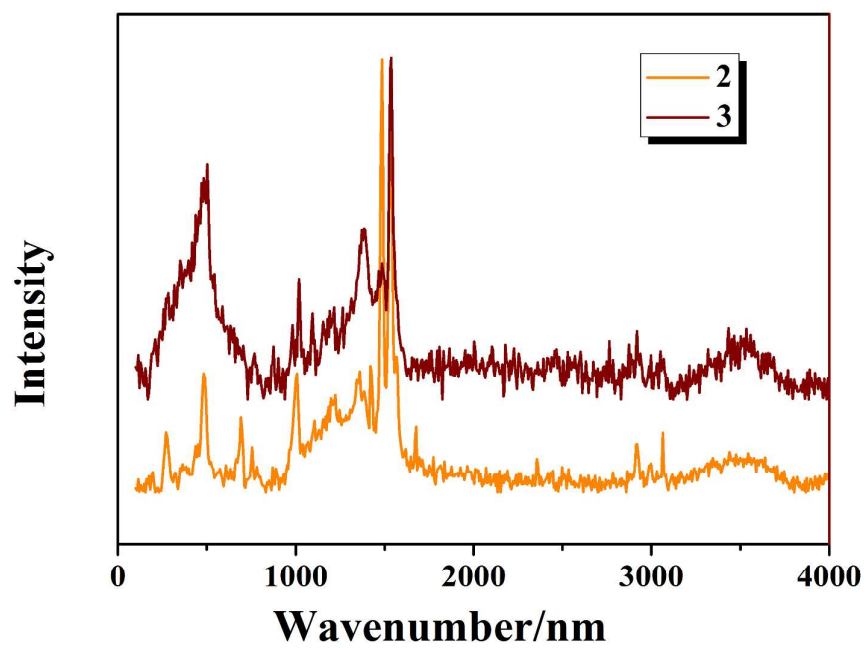
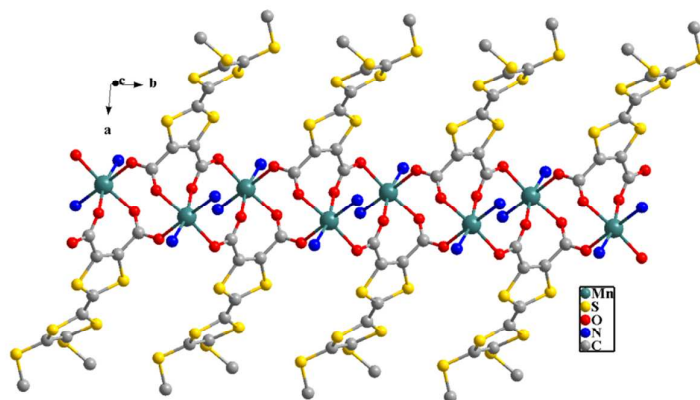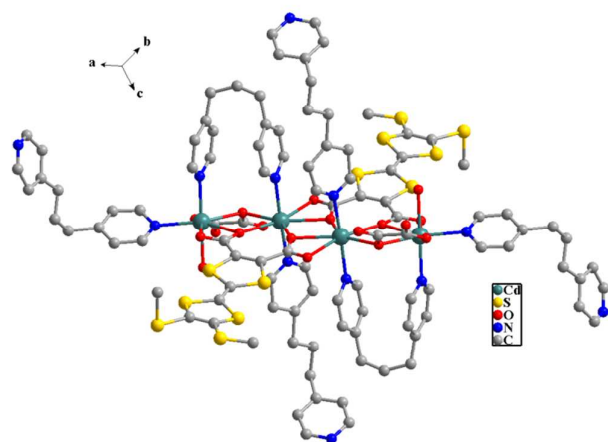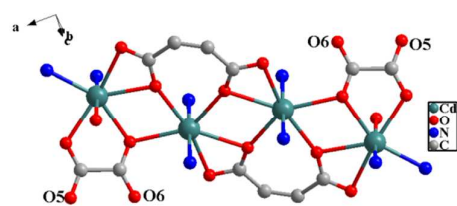Figure S3 Raman spectra for compounds **2** and **3**.

Figure S4 The chain structure bridged by L along the *b* axis of [MnL(bpp)]*n* (**1**), bpp is omitted for clarity.

(a)

(b)
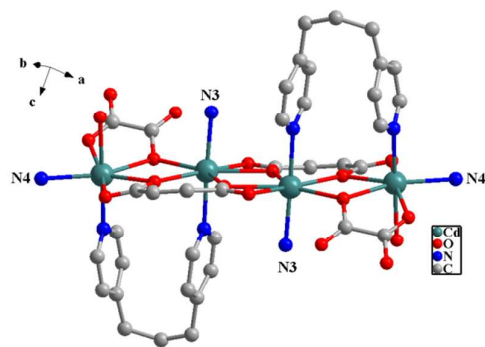
(c)
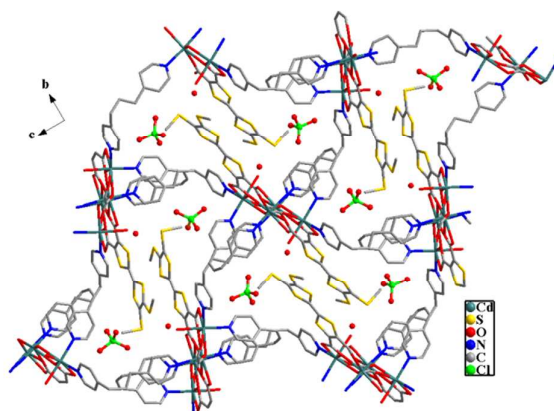
(d)

Figure S5 (a) Structure of $[Cd_2L(bpp)_2(H_2O)(C_2O_4)_{0.5}]_n \cdot n(ClO_4) \cdot n(H_2O)$ (**3**). (b) and (c) Centrosymmetric tetranuclear cluster through double μ_2-O bridges from two different L. (d) 3-D MOF structure showing that TTF dimers, perchlorate anions and water molecules are occupied in the pores.

Table S1. Crystal data and structural refinement parameters for **1**–**3**.

	1	2	3
formula	$C_{23}H_{20}MnN_2O_4S_6$	$C_{23}H_{20}MnN_2O_4S_6$	$C_{37}H_{38}Cd_2ClN_4O_{12}S_6$
fw	635.71	693.17	1183.32
cryst size (mm^3)	0.10×0.20×0.40	0.05×0.15×0.15	0.15×0.20×0.40
cryst syst	monoclinic	monoclinic	monoclinic
space group	$C2/c$	$C2/c$	$P2_1/n$
a (Å)	30.627(4)	30.933(8)	11.679(2)
b (Å)	7.4058(9)	7.3886(16)	16.526(3)
c (Å)	25.397(3)	25.700(7)	25.117(5)
α (deg)	90.00	90.00	90.00
β (deg)	111.391(3)	111.909(6)	90.02(3)
γ (deg)	90.00	90.00	90.00
V ($Å^3$)	5363.6(12)	5449(2)	4848.0(17)
Z	8	8	4
ρ_{calcd} (g cm^{-3})	1.574	1.690	1.621
$F(000)$	2600	2784	2372
μ (mm^{-1})	0.993	1.295	1.250
T (K)	293(2)	293(2)	293(2)
reflns collected	14878	12577	35447
unique reflns	6132	4652	8341
observed reflns	4450	3019	6384
no. params	328	323	546
GOF on F^2	1.130	1.194	1.141
R_1 [$I>2\sigma(I)$]	0.0769	0.1225	0.1259
wR_2 [$I>2\sigma(I)$]	0.1267	0.1802	0.1805